Available online at www.sciencedirect.com
ScienceDirect
Journal of Hazardous Materials 151 (2008) 616–622
Journal of Hazardous Materials
www.elsevier.com/locate/jhazmat

Removal of phosphate by mesoporous ZrO_2

Honglei Liu, Xiaofei Sun, Chengqing Yin, Chun Hu *

Research Center for Eco-Environmental Sciences, Chinese Academy of Sciences, Beijing 10085, China

Received 12 March 2007; received in revised form 8 June 2007; accepted 8 June 2007
Available online 14 June 2007

Abstract

A type of mesoporous ZrO_2 was synthesized and its phosphate removal potential was investigated in this study. The adsorption isotherm, pH effect, ionic strength effect and desorption were examined in batch experiments. The adsorption data fitted well to the Langmuir model with which the maximum P adsorption capacity was estimated to be 29.71 mg P/g. The amount of phosphate adsorbed increased rapidly in the first 5 h and slowly towards the end of the run, suggesting the possible monolayer coverage of phosphate ions on the surface of the adsorbent. The phosphate adsorption tended to increase with a decrease of pH and an increase of ionic strength. A phosphate desorbability of approximately 60% was observed with 0.5 M NaOH, which indicated a relatively strong bonding between the adsorbed PO_4^{3-} and the sorptive sites on the surface of the adsorbent. The immobilization of phosphate probably occurs by the mechanisms of ion exchange and physicochemical attraction. Due to its high adsorption capacity, this type of Zirconium oxide has the potential for application to control phosphorus pollution.

Keywords: Adsorption; Mesoporous; Phosphate; Zirconium

1. Introduction

The presence of trace amounts of phosphate in treated wastewaters from municipalities and industries can lead to eutrophication of the receiving confined water bodies [1]. So, the removal of phosphates from wastewater discharges to water bodies is an important component of eutrophication control strategies [2]. As regulations and standards become increasingly more stringent, from 0.5 to 1.0 mg/L to even less than 0.03 mg/L P, even further treatment of the effluent is required to meet effluent quality standards [3–5].

Among the conventional phosphorus removal methods, sorption methods using the appropriate solid materials can be promising at lower phosphate concentrations, which pose a challenge to the use of the traditional flocculation methods [6]. Most of the studies about phosphate adsorbents have focused on the choice of natural and constructed wetland system substrates, due to the importance of selecting substrates with the highest P adsorption capacity to maximize phosphorus removal [7].

Many kinds of materials have the potential to remove phosphorus from water, and many materials including waste products have attracted widespread interest due to their potential ability for phosphorus remove, including sands [8,9], fly ash [5,10–14], slag [11,14–18], iron oxide tailings [19], aluminum oxide hydroxide [20], Ca-based sorbents [21–24], alunite [25,26], red mud [27,28], and iron-based compounds [6,29].

Based on the risk of very dilute contaminants in water and more stringent standards imposed, it is important to develop new kinds of effective adsorbents [6,30]. Hydrous zirconium oxide has remarkable selectivity to phosphoric ions, and also high resistance against attacks by acids, alkalis, oxidants and reductants [31], which means that it has great potential to immobilize phosphate from water. In the present study, a type of mesoporous ZrO_2 was synthesized, and its phosphate removal property as a function of pH, contact time and ionic strength was studied.

2. Materials and methods

2.1. Materials

Mesoporous ZrO_2 was synthesized via solid-state reaction using a structure-directing method [32]. In this synthesis, $ZrOCl_2{\cdot}8H_2O$ and NaOH were milled into fine powder,

* Corresponding author. Tel.: +86 10 62849171; fax: +86 10 62923541.
E-mail address: huchun@rcees.ac.cn (C. Hu).

0304-3894/$ – see front matter © 2007 Elsevier B.V. All rights reserved.
doi:10.1016/j.jhazmat.2007.06.033

respectively, and mixed at ambient temperature with the assistance of block-copolymer $HO(CH_2CH_2O)_X(CH_2CH(CH_3)O)_Y(CH_2CH_2O)_XH$ (fw = 5800). The mixture was then transferred into an autoclave and kept at 383 K for 48 h. Subsequently, the compound was washed first with water, and then with ethanol. After this, it was dried at 350 °C for 3 h before use.

Commercial ZrO_2 was also studied as a reference. Standard phosphate solutions were prepared by dissolving the anhydrous potassium dihydrogen orthophosphate (KH_2PO_4) and KNO_3 in appropriate amounts of distilled water. The pH value of the PO_4^{3-} working solution was adjusted to neutral with diluted HCl or KOH.

2.2. Effect of contact time

The influence of time was assessed by reacting 450 ml of a phosphate solution (30 mg P/L and 0.01 M KNO_3) with 600 mg mesoporous ZrO_2 powder for up to 24 h, with the commercial ZrO_2 as reference. The flask was covered and immediately stirred. Several mL of reaction solution was sampled with a pipettor at various time intervals between 0 and 24 h of adsorption. The pH level was also measured at the same time. The sample solution was immediately filtered through a 0.45 μm membrane filter, and the filtrate was taken for PO_4^{3-} analysis. Plots were prepared between the percentages of phosphate removed versus time. Finally, the exhausted sorbents were taken out for further desorption studies.

2.3. Adsorption isotherms

Triplicate 60 mg samples of mesoporous ZrO_2 were placed in 50 mL of 0.01 M KNO_3 containing different amounts of P as KH_2PO_4. Three drops of chloroform were added to each tube to inhibit bacteria growth. Seven levels of initial phosphate concentrations (0, 5, 10, 20, 30, 50, 100, 200 and 300 mg P/L) were used. The experiments were performed using 0.01 M KNO_3 to adjust the ionic strength, independently of the amount of KH_2PO_4 added. The pH value of the PO_4^{3-} working solution was adjusted to the equilibrium value by adding KOH or HNO_3 in order to minimize pH variations due to the different amounts of KH_2PO_4 added. The suspensions were continually shaken at room temperature (25 °C) and 180 rpm for 24 h to ensure approximate equilibrium. The supernatant was filtered by a 0.45 μm filter paper and then was analyzed for P using a Perkin-Elmer Elan 6000 ICP-OES. The quantity of adsorbed phosphate (adsorption capacity) was calculated from the decrease of the phosphate concentration in solutions.

Then the P sorption data were fitted to the Langmuir equation shown below:

$$\frac{1}{q_e} = \frac{1}{Q} + \frac{1}{bQ} * \frac{1}{C_e} \quad \text{(Langmuir isotherm)}$$

Detailed definitions of the variables can be found in the literature [19]. The exhausted adsorbents were taken out for IR spectrum determination.

2.4. Effect of pH and ionic strength

To study the influence of pH and ionic strength on the adsorption capacity, experiments were performed by using four solutions of 30 mg P/L (0.001, 0.01 and 0.1 M KNO_3) reacting with 600 mg adsorbent while maintaining the pH at different values between 3 and 11. The flasks were shaken continuously for 24 h to attain equilibrium, after which the residual concentration of phosphate in the supernatant solutions was determined.

2.5. Desorption studies

To evaluate phosphate desorption from the exhausted adsorbent, the residual solids retained on the filter paper were collected after filtration of the suspension from the above test. To each flask containing 50 mg of exhausted mesoporous ZrO_2, 50 mL of 0.01 M KCl solution with different KOH (0, 0.001, 0.01, 0.1 and 0.5 M) was added. The flasks were then shaken for 24 h. The suspension solutions were filtered and analyzed for phosphate as according to the method described previously. The quantity of desorbed phosphate was determined by the amount of phosphate in the solution after the desorption experiment. The P desorbability was defined as the ratio of the desorbed P over the total P adsorbed by the adsorbent.

2.6. Other physicochemical measurements

The solids' structures were analyzed by X-ray diffraction (XRD) using Cu Kα radiation (Rint 2500, Rigaku). Their morphology and microstructures were measured with Scanning Electronic Microscopy (SEM) technique (S-3000N, Hitachi) and BET protocol (BELSORP-mini, BEL Japan). The IR spectra of ZrO_2 were taken before and after the adsorption tests on a Nicolt IR-5700 spectrophometer as KBr pellets in the range of 4000–400 cm^{-1}. The zeta potential of ZrO_2 was determined using the method of [33].

3. Results and discussion

3.1. Properties of synthesized mesoporous adsorbent

The X-ray diffraction pattern of the commercial and synthesized mesoporous ZrO_2 are shown in Fig. 1a and b, respectively. According to the literature [34], the synthesized adsorbent consists mainly of a tetragonal phase with the commercial ZrO_2 being monoclinic. SEM analysis (Fig. 2a and b) proved the amorphous state of these commercial and synthesized ZrO_2. Fig. 3b is the N_2 adsorption/desorption isotherm. When subjected to N_2 gas desorption, the isotherm revealed a hysteretic behavior for the synthesized adsorbent. The hysteresis observed at higher relative pressures (>0.5) suggested the abundance of mesopores in the adsorbent [35]. The BET specific surface area was 232 m^2/g and the pore diameter was ~3.9 nm. As a reference, the commercial ZrO_2 was also characterized by nitrogen adsorption/desorption isotherms (Fig. 3a). The results indicated that the commercial counterpart was nonporous with the specific surface area of 8.83 m^2/g.

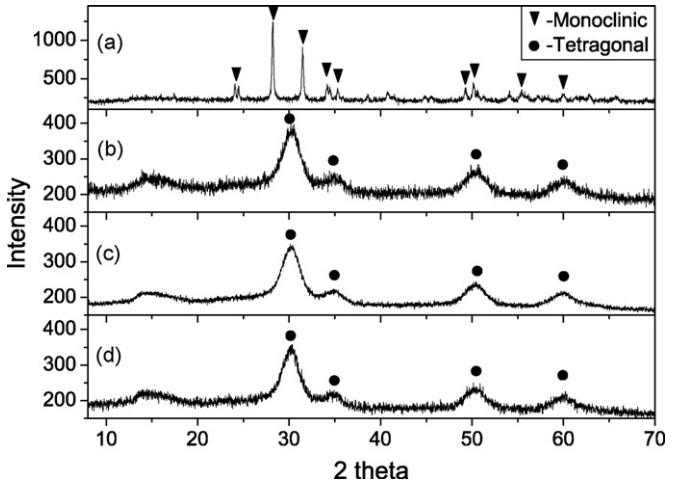

Fig. 1. X-ray diffraction patterns of commercial (a), mesoporous ZrO_2 before treatment (b), mesoporous ZrO_2 treated with 5 ppm PO_4^{3-} solution (c) and mesoporous ZrO_2 treated with 50 ppm PO_4^{3-} solution (d).

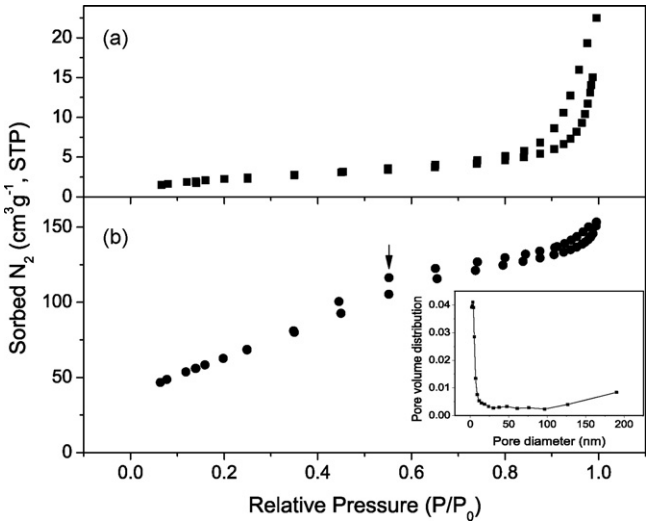

Fig. 3. Changes in N_2 gas adsorption/desorption isotherm of mesoporous ZrO_2.

3.2. *Effect of contact time*

Fig. 4 depicts the percentage of phosphate removed versus time for both the synthesized adsorbent and the commercial reference adsorbent. The pH value is also shown in this figure. The reference powder had a much lower phosphate adsorption potential than the mesoporous counterpart. For the commercial ZrO_2, the phosphate removal ratio was less than 7% after 24 h, and the pH stayed constant throughout the whole reaction time. However, for the mesoporous ZrO_2, Fig. 4 shows that the amount of phosphate adsorbed increased rapidly in the beginning 5 h and slowly towards the end of the run. At the time of 5 h, about 54.4% of the phosphate in the solution had been removed. The remaining 19 h only added about another 4.4% to the phosphate removal ratio. The results in Fig. 4 also show that the pH value fluctuation coincides with the amount of phosphate immobi-

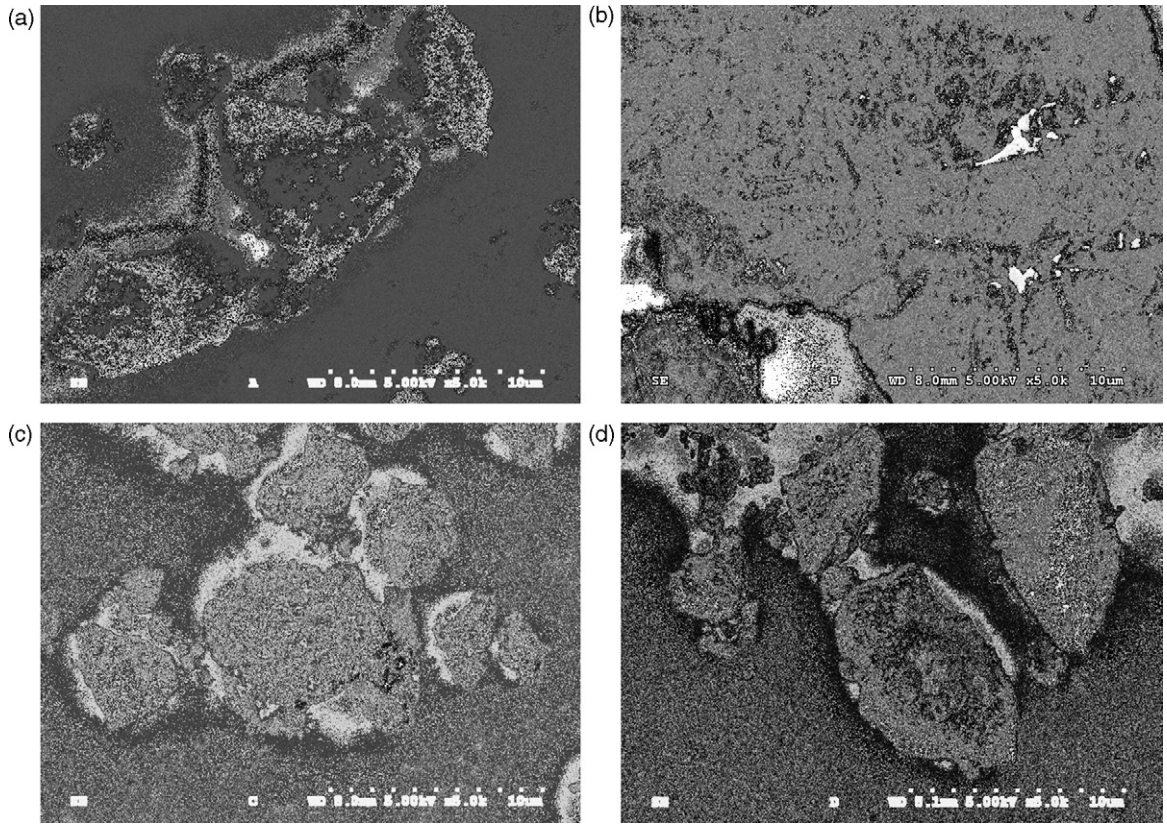

Fig. 2. SEM analysis of commercial (a), mesoporous ZrO_2 before treatment (b), mesoporous ZrO_2 treated with 5 ppm PO_4^{3-} solution (c) and mesoporous ZrO_2 treated with 50 ppm PO_4^{3-} solution (d).

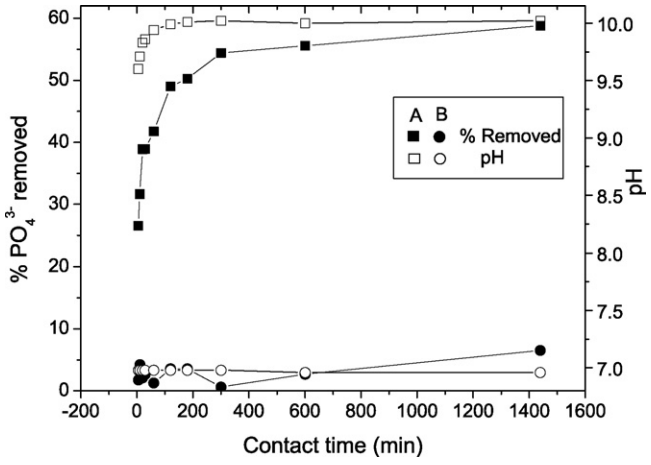

Fig. 4. Rate of phosphate removal and equilibrated pH from the 450 mL solution of 30 mg P/L by 0.600 g adsorbents at 25 °C (A: synthesized mesoporous ZrO_2; B: commercial ZrO_2).

lized. The value of pH in the solution increased rapidly from 9.60 at the time of 5 min to 10.02 at the time of 5 h, and then remained constant for the rest of the run time.

3.3. Adsorption isotherm

Fig. 5 shows a plot of the phosphate loading on the adsorbent against the phosphate equilibrium concentration in the liquid phase. It was found that the Langmuir equation best described the equilibrium data over the concentration range used in this investigation ($r^2 = 0.965$). With this Langmuir equation, the maximum P adsorption capacity was estimated to be 29.71 mg P/g.

The adsorption isotherm can indicate how the adsorbate molecules are distributed between the liquid phase and the solid phase when the adsorption process reaches an equilibrium state [24]. The good fit of the Langmuir equation to the adsorption isotherm indicates that the precipitation of zirconium phosphate can be negligible, as the Langmuir equation can only be used to describe the adsorption processes without precipitation [9]. Although the Langmuir Q value might not provide an accurate estimation of the long-term sorption capacity, it could still be useful in comparing alternative materials for wastewater treatment [13]. The adsorption capacity of 29.7 mg/g shows that this mesoporous ZrO_2 has relatively high potential to be used as a phosphate adsorbent in treating effluents.

3.4. Other physicochemical determinations

X-ray diffraction patterns, SEM analysis of mesoporous ZrO_2 before and after treated with PO_4^{3-} solutions are shown in Figs. 1–3, respectively. It is found from Figs. 1 and 2 that the treatment with phosphate solution neither changes the crystalline phase nor leads to any new crystalline phases.

The BET analysis showed that after treated with PO_4^{3-} solutions (5 or 50 ppm), the specific area of mesoporus ZrO_2 was still around 230 m^2/g and no significant change was found for the pore diameter distribution. These results indicated that the amount of phosphate adsorbed was far less than fulfilling the major pores of the adsorbent.

The results of zeta potential and IR spectra determination are presented in Figs. 6 and 7, respectively. Fig. 6 shows that the isoelectric point was at pH 4.9. Below pH 4.9 the particles acquire a positive charge. Above pH 4.9 the charge of the adsorbent is negative, and it increases with pH.

In the IR spectrum of mesoporous ZrO_2 before adsorption, a strong and broad band in the 3500–3300 cm^{-1} region (O–H stretching vibration) and a band at 1590 cm^{-1} (O–H bending vibration) indicated the presence of coordinated water molecules, with the peak at 1340 cm^{-1} (O–H bending vibration) indicating the presence of surface hydroxyl on the metal oxide surface. It could be seen that after adsorption, the peaks at both 1590 and 1340 cm^{-1} were shifted to a high wavenumber zone (1625 and 1380, respectively) and weakened dramatically. The decreasing tendency of these two peaks indicated that most of the surface hydroxyl groups were replaced by adsorbed PO_4^{3-}. The peak appearing at 1015 cm^{-1} was attributed to the bending

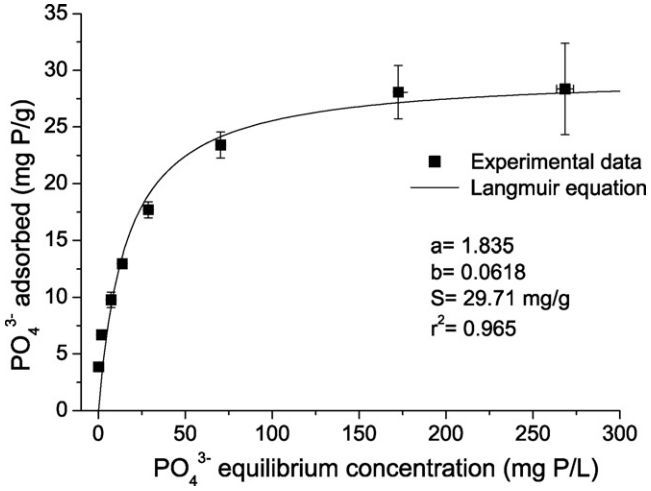

Fig. 5. Phosphate adsorption isotherm of mesoporous ZrO_2 at 20 °C and pH 6.7–6.9.

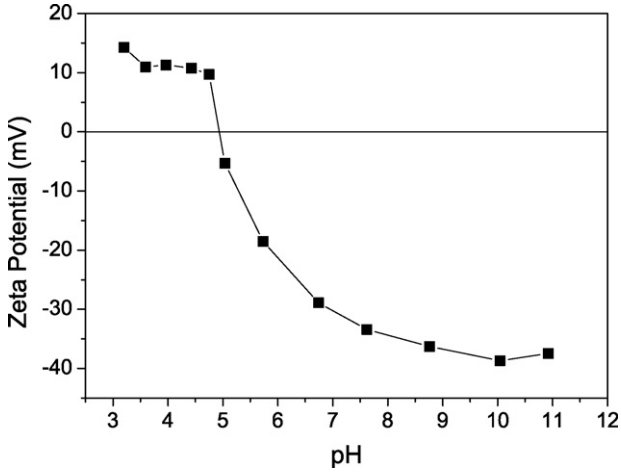

Fig. 6. Plot of the zeta potential of mesoporous ZrO_2 as a function of pH at 0.01 M NaCl, 25 °C.

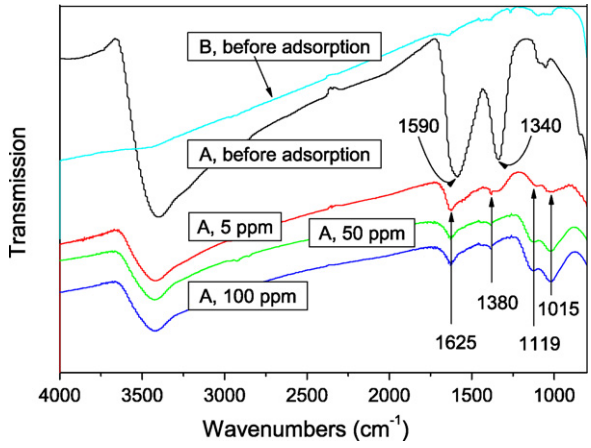

Fig. 7. The IR spectra of ZrO_2 before and after adsorption, (A: commercial ZrO_2; B: synthesized mesoporous ZrO_2).

vibration of adsorbed PO_4^{3-}. At the same time, a weak shoulder peak appeared at 1119 cm^{-1}. For the commercial ZrO_2, the lack of any peaks at around 1340 cm^{-1} indicated that there was no surface hydroxyl on the metal oxide surface. This accounted for the fact that the phosphate adsorption on the commercial ZrO_2 powder was very low, with no pH changes during the run time.

3.5. Effect of pH and ionic strength

As demonstrated by the results obtained from the pH and ionic strength influence test (shown in Fig. 8), the efficiency of PO_4^{3-} removal increased steadily with the decrease of pH. For the system with 0.001 M KNO_3, at pH 10.18, the amount of phosphate loaded on the adsorbent was only 11.97 mg P/g. However, at pH 2.82, this amount reached 23.29 mg P/g, approximately twice as much as the value at pH 10.18. Fig. 8 also shows the effect of ionic strength on the phosphate adsorption. The phosphate adsorption was slightly dependent on the ionic strength, especially in the high pH range.

Electrolytes can form outer-sphere complexes through electrostatic forces [36]. So, if the immobilization of phosphate

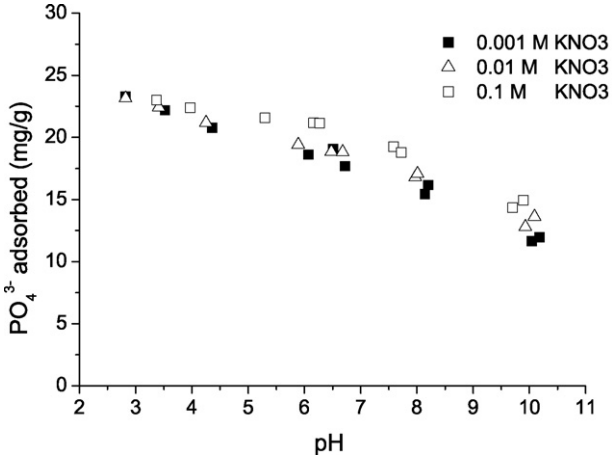

Fig. 8. Effect of pH and ionic strength on phosphate adsorption on mesoporous ZrO_2.

ions occurs through the formation of outer-sphere surface complexes, the removal ratio will decrease with an increase of ionic strength. For this mesoporous ZrO_2, the percentage of phosphate removed did not decrease with the increase of ionic strength, which indicates that the immobilization of phosphate ions probably takes place through the formation of inner-sphere surface complexes at the water/oxide surface. The pH dependency must be related to both the amphoteric properties of the ZrO_2 surface and to the polyprotic nature of phosphate. The surface of ZrO_2 consists mainly of oxygen atoms and hydroxyl groups. It is primarily the hydroxyl groups that determine the chemistry (acid–base characteristics) and the reactivity of such metal (hydro)oxide surfaces [24,37]. The acidic phosphates ($H_2PO_4^-$ and HPO_4^{2-}) are the predominant aqueous species for the pH range of 3–9 [12]. At this pH range, phosphate removal probably occurs with ion exchange mechanisms of phosphate hydrolysis products ($H_2PO_4^-$, HPO_4^{2-}) on the surface of ZrO_2 as follows (Eqs. (1) and (2)):

$$Zr\text{–}OH + H_2PO_4^- = Zr(H_2PO_4) + OH^- \quad (1)$$

$$2Zr\text{–}OH + HPO_4^{2-} = Zr_2(HPO_4) + 2OH^- \quad (2)$$

This assumption agrees with the finding based on the IR spectra that most of the surface hydroxyl groups disappear after adsorption. This also confirms the increase in the pH of the equilibrium solution accompanied with the immobilization of P.

According to the literature [29], when the pH is below the isoelectric point, the surface hydroxyl is protonated (Eq. (3)) and positively charged. Then the electrostatic attraction between the negative phosphate anions and the positive protonated ZrO_2 surface will occur (Eq. (4) and (5)).

$$Zr\text{–}OH + H^+ = Zr\text{–}OH_2^+ \quad (3)$$

$$Zr\text{–}OH_2^+ + H_2PO_4^- = (Zr\text{–}OH_2)^+(H_2PO_4)^- \quad (4)$$

$$2Zr - OH_2^+ + HPO_4^{2-} = (Zr\text{–}OH_2)_2^+(HPO_4)^{2-} \quad (5)$$

Fig. 8 shows that the more acidic the solution, the more P would be removed, which indicated that the physicochemical adsorption due to Coulombic attraction was the predominant process of P removal. In the lower pH range, Coulombic attraction can readily occur in conjunction with specific chemical adsorption due to an exchange reaction [20]. However, with an increase of pH, the protonated surface sites will continue to decrease. The phosphate removal was lower at higher pH values probably because of stronger competition with hydroxide ions on the adsorbent surface [18], and the increased repulsion between the more negatively charged PO_4^{3-} species and negatively charged surface sites [19].

Fig. 8 shows that the immobilization of phosphate was slightly enhanced by an increase of ionic strength. This phenomenon is similar to the findings using other metal oxides [38,39]. Two consequences of the increase of ionic strength can account for this enhancement.

First, the H^+ in the Zr–OH hydroxyl on the adsorbent surface can be replaced with K^+ from the electrolyte solution KNO_3 (Eq. (6)). Since K^+ is adsorbed with the equivalent release of H^+, the increase in the concentration of H^+ tends to decrease the

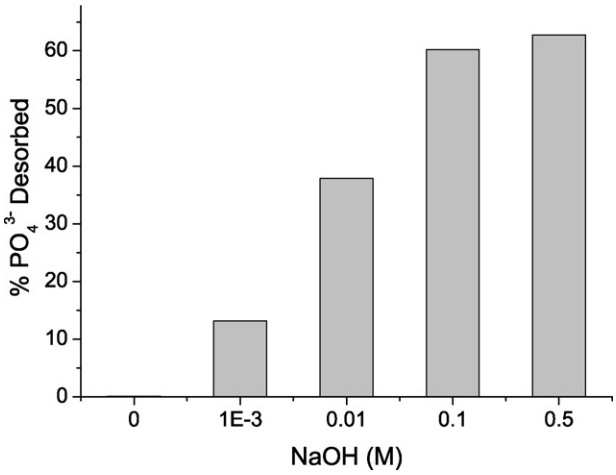

Fig. 9. The ratio of phosphate desorbed from used mesoporous ZrO_2.

pH_f (pH at final time). This was confirmed by the lower pH_f that resulted from the high electrolyte concentrations in the solution (Fig. 8).

$$Zr–OH + K^+ = Zr–OK + H^+ \quad (6)$$

Some of the equivalent H^+ released can then be adsorbed to the other Zr–OH hydroxyl on the adsorbent surface (Eq. (3)). The protonated ZrO_2 surface will inevitably promote the phosphate adsorption capability (Fig. 8).

Second, electrolytes such as the iron oxides [40], and struvite [30] may influence the surface charges directly. The electric charge of the particles in their suspensions plays an important role in the particle–particle interactions, which will in turn affect phosphate adsorption on the adsorbent surface.

3.6. Desorption studies

According to the results of desorption studies (Fig. 9), the amount of the desorbed P increased with the increase of alkalinity. When no NaOH was added, the solution of 0.01 M KCl only extracted 0.13% phosphate immobilized on the adsorbent surface. If the alkalinity reached 0.1 M, more than 60% could be liberated into the liquid. Much higher alkalinity (0.5 M) did not lead to a corresponding higher desorption ratio than at 0.1 M NaOH (Fig. 9).

The results of these desorption studies indicate that the P adsorption on the ZrO_2 is not completely reversible and the bonding between the tailings particles and adsorbed PO_4^{3-} is probably strong. It is relatively difficult for the adsorbed PO_4^{3-} to be desorbed from the ZrO_2. The implication of these results is that this mesoporous ZrO_2 has the potential to be used as an adsorbent for phosphate removal from wastewater.

4. Conclusion

The data for the adsorption of phosphate onto mesoporous ZrO_2 fit the Langmuir model well. The immobilization of phosphate was slightly enhanced by an increase of ionic strength. The immobilization of phosphate probably occurs by the mechanisms of ion exchange and physicochemical attraction. The results of this study showed that this mesoporous ZrO_2 has a much better phosphate removal capability than the commercial reference. Due to its high capability, this type of zirconium oxide has the potential to control phosphorus pollution, and the mechanisms deduced here may help to further modify of this material to improve the phosphate removal potential.

Acknowledgement

We are grateful to Gaosheng Zhang for language correction and discussions. This work was supported by National Natural Science Foundation of China (No. 50621804, 50538090, 20537020), and National Basic Research Priorities Programs (2006CB403306 and 2002CB42308).

References

[1] E. Oguz, A. Gurses, N. Canpolat, Removal of phosphate from wastewaters, Cem. Concr. Res. 33 (2003) 1109–1112.
[2] H.B. Kwon, C.W. Lee, B.S. Jun, J.D. Yun, S.Y. Weon, B. Koopman, Recycling waste oyster shells for eutrophication control, Resour. Conserv. Recy. 41 (2004) 75–82.
[3] D.Y. Zhao, A.K. Sengupta, Ultimate removal of phosphate from wastewater using a new class of polymeric ion exchangers, Water Res. 32 (1998) 1613–1625.
[4] L.J. Puckett, Identifying the major sources of nutrient water-pollution, Environ. Sci. Technol. 29 (1995) A408–A414.
[5] A. Ugurlu, B. Salman, Phosphorus removal by fly ash, Environ. Int. 24 (1998) 911–918.
[6] Y. Seida, Y. Nakano, Removal of phosphate by layered double hydroxides containing iron, Water Res. 36 (2002) 1306–1312.
[7] H. Brix, Use of constructed wetlands in water-pollution control—historical development, present status, and future perspectives, Water Sci. Technol. 30 (1994) 209–223.
[8] C.A. Arias, M. Del Bubba, H. Brix, Phosphorus removal by sands for use as media in subsurface flow constructed reed beds, Water Res. 35 (2001) 1159–1168.
[9] M. Del Bubba, C.A. Arias, H. Brix, Phosphorus adsorption maximum of sands for use as media in subsurface flow constructed reed beds as measured by the Langmuir isotherm, Water Res. 37 (2003) 3390–3400.
[10] O. Khelifi, Y. Kozuki, H. Murakami, K. Kurata, M. Nishioka, Nutrients adsorption from seawater by new porous carrier made from zeolitized fly ash and slag, Mar. Pollut. Bull. 45 (2002) 311–315.
[11] N.M. Agyei, C.A. Strydom, J.H. Potgieter, An investigation of phosphate ion adsorption from aqueous solution by fly ash and slag, Cem. Concr. Res. 30 (2000) 823–826.
[12] D.G. Grubb, M.S. Guimaraes, R. Valencia, Phosphate immobilization using an acidic type F fly ash, J. Hazard. Mater. 76 (2000) 217–236.
[13] K.C. Cheung, T.H. Venkitachalam, Improving phosphate removal of sand infiltration system using alkaline fly ash, Chemosphere 41 (2000) 243–249.
[14] N.M. Agyei, C.A. Strydom, J.H. Potgieter, The removal of phosphate ions from aqueous solution by fly ash, slag, ordinary Portland cement and related blends, Cem. Concr. Res. 32 (2002) 1889–1897.
[15] K. Sakadevan, H.J. Bavor, Phosphate adsorption characteristics of soils, slags and zeolite to be used as substrates in constructed wetland systems, Water Res. 32 (1998) 393–399.
[16] L. Johansson, Blast furnace slag as phosphorus sorbents—column studies, Sci. Total Environ. 229 (1999) 89–97.
[17] L. Johansson, J.P. Gustafsson, Phosphate removal using blast furnace slags and opoka-mechanisms, Water Res. 34 (2000) 259–265.
[18] E. Oguz, Removal of phosphate from aqueous solution with blast furnace slag, J. Hazard. Mater. 114 (2004) 131–137.
[19] L. Zeng, X.M. Li, J.D. Liu, Adsorptive removal of phosphate from aqueous solutions using iron oxide tailings, Water Res. 38 (2004) 1318–1326.

[20] S. Tanada, M. Kabayama, N. Kawasaki, T. Sakiyama, T. Nakamura, M. Araki, T. Tamura, Removal of phosphate by aluminum oxide hydroxide, J. Colloid Interf. Sci. 257 (2003) 135–140.
[21] S. Karaca, A. Gurses, M. Ejder, M. Acikyildiz, Adsorptive removal of phosphate from aqueous solutions using raw and calcinated dolomite, J. Hazard. Mater. 128 (2006) 273–279.
[22] A.S. Brooks, M.N. Rozenwald, L.D. Geohring, L.W. Lion, T.S. Steenhuis, Phosphorus removal by wollastonite: a constructed wetland substrate, Ecol. Eng. 15 (2000) 121–132.
[23] M. Khadhraoui, T. Watanabe, M. Kuroda, The effect of the physical structure of a porous Ca-based sorbent on its phosphorus removal capacity, Water Res. 36 (2002) 3711–3718.
[24] D.C. Southam, T.W. Lewis, A.J. McFarlane, J.H. Johnston, Amorphous calcium silicate as a chemisorbent for phosphate, Curr. Appl. Phys. 4 (2004) 355–358.
[25] M. Ozacar, Phosphate adsorption characteristics of alunite to be used as a cement additive, Cem. Concr. Res. 33 (2003) 1583–1587.
[26] M. Ozacar, Contact time optimization of two-stage batch adsorber design using second-order kinetic model for the adsorption of phosphate onto alunite, J. Hazard. Mater. 137 (2006) 218–225.
[27] B. Koumanova, M. Drame, M. Popangelova, Phosphate removal from aqueous solutions using red mud wasted in bauxite Bayer's process, Resour. Conserv. Recy. 19 (1997) 11–20.
[28] G. Akay, B. Keskinler, A. Cakici, U. Danis, Phosphate removal from water by red mud using crossflow microfiltration, Water Res. 32 (1998) 717–726.
[29] O. Bastin, F. Janssens, J. Dufey, A. Peeters, Phosphorus removal by a synthetic iron oxide-gypsum compound, Ecol. Eng. 12 (1999) 339–351.
[30] J.D. Doyle, S.A. Parsons, Struvite formation, control and recovery, Water Res. 36 (2002) 3925–3940.
[31] T.M. Suzuki, J.O. Bomani, H. Matsunaga, T. Yokoyama, Preparation of porous resin loaded with crystalline hydrous zirconium oxide and its application to the removal of arsenic, React. Funct. Polym. 43 (2000) 165–172.
[32] X.M. Liu, G.Q. Lu, Z.F. Yan, Synthesis and stabilization of nanocrystalline zirconia with MSU mesostructure, J. Phys. Chem. B 108 (2004) 15523–15528.
[33] N.C. Bouropoulos, P.G. Koutsoukos, Spontaneous precipitation of struvite from aqueous solutions, J. Cryst. Growth 213 (2000) 381–388.
[34] Z. Qian, J.L. Shi, Characterization of pure and doped ziroconia nanoparticles with infrared transmission spectroscopy, Nanostruct. Mater. 10 (1998) 235–244.
[35] K.C. Makris, W.G. Harris, G.A. O'Connor, H. El-Shall, Long-term phosphorus effects on evolving physicochemical properties of iron and aluminum hydroxides, J. Colloid Interf. Sci. 287 (2005) 552–560.
[36] T.H. Hsia, S.L. Lo, C.F. Lin, D.Y. Lee, Characterization of arsenate adsorption on hydrous iron-oxide using chemical and physical methods, Colloid Surf. A 85 (1994) 1–7.
[37] Y. Al-Degs, M.A.M. Khraisheh, S.J. Allen, M.N. Ahmad, Effect of carbon surface chemistry on the removal of reactive dyes from textile effluent, Water Res. 34 (2000) 927–935.
[38] M.T. Pardo, M.E. Guadalix, M.T. Garciagonzalez, Effect of pH and background electrolyte on P sorption by variable charge soils, Geoderma 54 (1992) 275–284.
[39] R. Giesler, T. Andersson, L. Lovgren, P. Persson, Phosphate sorption in aluminum- and iron-rich humus soils, Soil Sci. Soc. Am. J. 69 (2005) 77–86.
[40] J.C. Ryden, J.R. Mclaughlin, J.K. Syers, Mechanisms of phosphate sorption by soils and hydrous ferric oxide gel, J. Soil Sci. 28 (1977) 72–92.